CHALMERS

Automatic Generation of Radial Ball Bearing FE-Models

Master's Thesis in Solid and Fluid Mechanics

PETTER HOLMBERG
PRAVIN UGALE

Department of Applied Mechanics
Division of Dynamics
CHALMERS UNIVERSITY OF TECHNOLOGY
Göteborg, Sweden 2011
Master's Thesis 2011:52

MASTER'S THESIS 2011:52

Automatic Generation of Radial Ball Bearing FE-Models

Master's Thesis in Solid and Fluid Mechanics

PETTER HOLMBERG
PRAVIN UGALE

Department of Applied Mechanics
Division of Dynamics
CHALMERS UNIVERSITY OF TECHNOLOGY
Göteborg, Sweden 2011

Automatic Generation of Radial Ball Bearing FE-Models
PETTER HOLMBERG
PRAVIN UGALE

Master's Thesis 2011:52
ISSN 1652-8557
Department of Applied Mechanics
Division of Dynamics
Chalmers University of Technology
SE-412 96 Göteborg
Sweden
Telephone: + 46 (0)31-772 1000

Chalmers Reproservice
Göteborg, Sweden 2011

Automatic Generation of Radial Ball Bearing FE-Models
Master's Thesis in Solid and Fluid Mechanics
PETTER HOLMBERG
PRAVIN UGALE
Department of Applied Mechanics
Division of Dynamics
Chalmers University of Technology

Abstract

In Finite Element (FE) analyses of transmission components such as gearboxes or differentials, there is a need for accurate bearing models to predict the behavior and properties of the system. The models also needs to be easy to implement and generate, and relatively simple to be fast and stable. This thesis deals with the radial ball bearings specifically.

Initial literature studies found it suitable to model the outer ring with solid elements and the inner ring with either solid elements or a rigid body from the rolling elements to the load center. The rolling element were replaced with nonlinear elastic springs with stiffness calculated based on Hertz contact theory to capture the contact zones deformation which is the most significant factor to the overall bearing stiffness.

For the model to be easy to create, a script was written in Python to generate an ABAQUS input file from bearing properties specified in a text file for radial ball bearings. The input file for the bearing can then be loaded and implemented into a larger FE-model.

Main focus of the thesis was to create a functional script that would generate a stable and reliable radial ball bearing model that could be used and relatively easy be modified for future needs. The model performs well with respect to convergency and low calculation times. Unfortunately the stiffness is much lower than measured results from real bearings. A close look at the deformation of the ring raceways gives us a reason to believe that this is because our springs are attached in a single node to the raceway and thus giving us a contact point to where all the transfered load between the rings is concentrated in, instead of a contact area as in a real bearing.

Keywords: radial ball bearing, ABAQUS, python script, automatic FE-model generation, Hertz contact theory

Contents

Acknowledgement

We would like to thank our examiner Håkan Johansson and our supervisor Gustav Caesar for their help during the project. We would also like to thank Johan Cederlund, Jon Elfridsson and Lina Roos at Xdin Analytix for help with various questions. Also Peter Falk, Tommie Hall and Ola Nilsson at GETRAG FORD Transmissions in Gothenburg and Anton Jurinic and Ulf Karlsson from SIMULIA Scandinavia/ABAQUS.

Göteborg September 2011
Petter Holmberg, Pravin Ugale

1 Introduction

Different types of bearings are used in many applications, especially in transmission components like gearboxes and differentials. The function and behavior of these components are very much affected by the stiffness of each bearing used and it is therefore important to have correct models of the bearings themselves. A work method to manually create a tapered roller bearing existed at the start of this thesis and were used at the Xdin office in FE-analyses of different transmission components. Tapered roller bearings is the most common bearing type in these kind of applications today, but there is an increasing interest for ball bearings since they have lower internal friction. The lower friction is one step to reach the demands of reduced vehicle emissions in which the transmission components are used.

An efficient method to generate FE-models for radial ball bearings was therefore needed and since creating a bearing manually each time a different bearing size is needed, it was decided that the work method should be made in to a Python script that automatically could generate an arbitrary radial ball bearing geometry based on input parameters such as geometrical dimensions and desired mesh density. This also guarantees that all bearings would be created in the same way independent on who the user is.

Rolling elements can be modeled as a solid elements as well. But this method requires finely refined mesh in the contact area and contact properties needs to be defined accurately in order to get realistic results. Model becomes expensive in terms of computation time and memory. This type of model is helpful to analyse the behaviour of contact area in details but there is no big advantage when it comes to modelling the stiffness of bearing itself in a transmission assembly. Hence it is practically advantageous to model rolling elements by nonlinear elastic springs that represents the contact deformations between the rolling elements and raceway surface in the bearing rings. A similar method was used by Chunjun [1] who used beams instead of springs in an angular contact ball bearing, and Golbach [4] who used a custom user element representing springs in a roller bearing and angular contact ball bearing. These deformations is what affects the bearing stiffness the most and is calculated with equations based on Hertz theory of contact mechanics [6]. The bearing outer ring would be created using solid elastic brick elements to make it easy to use in a larger FE-model, and the inner ring could be modeled either with solid elements as well or by a rigid body with reference point in the bearing center.

1.1 Objectives and limitations

The objective of this work is to create a script in Python programming language that will generate an efficient ABAQUS model for a radial ball bearing, also called deep groove ball bearing. The script shall be able to produce a model for an arbitrary bearing and be functional in standard static analyses as well as in large deformation analyses (NLGEOM) and eigenfrequency analyses.

The script will not be able to implement thermal expansion or second order elements into the models, but be relatively easy to modify in future work to add this.

1.2 Work plan

The project starts with literature studies of the contact mechanics of ball bearings to find a formulation for the contact deformations. At the same time a script is made in Python programming language that will create the bearing itself as an ABAQUS inputfile. The stiffness of the springs that represents the rolling elements can then be modified based on the deformation formulations obtained from the literature studies. When the script is finished and creates a satisfactory bearing model it will be tested to check for convergence stability, overall stiffness, and mesh density dependency. The script files will also be packed to an .exe container to make it possible to run even on a computer without Python installed.

2 Contact modeling of ball bearings

2.1 Introduction

A bearing basically consists of an outer and inner ring with a number of rolling elements placed between the two rings. When load is applied on the bearing the rolling elements are squeezed between the two rings and transfer compression force from one ring to the other. The rolling elements can not transfer tension loads, this means that if the compression load on any of them would decrease to zero it will be unloaded.

When the rolling element is compressed between the two rings, a contact zone will form where they come in contact with each other. This zone will grow as the load increases and the ring and rolling element is deformed within the contact zone. These local deformations occurring within the contact zones affects the overall bearing stiffness to a high degree. To get an accurate FE-model of the bearing it is therefore neccesary to calculate first the local deformations in each roller depending on the applied load and then combine them to get the global stiffness of the bearing.

The following section describes how this is achieved based on Hertz contact deformation theory of two bodies in contact [6].

2.2 Hertz contact theory

"Two bodies of revolution having different radii of curvature in a pair of principal planes passing through the contact between the bodies may contact each other at a single point under the condition of no applied load. Such a condition is called point contact." (Harris [5]). Figure 2.1 shows two such bodies where a pair of principal planes pass through the contact point. The first index of the radius of curvature denotes the body it belongs to, and the second index which plane. Hence r_{II2} is the radius of curvature of the second body in the second plane. The curvature is defined as

$$\rho = \frac{1}{r} \tag{2.1}$$

The radius of curvature is always positive but the curvature itself can be both positive and negative, with positive curvature for convex surface and negative curvature for concave surface.

The curvature sum $\Sigma\rho$ and curvature difference $F(\rho)$ can be introduced to describe the contact between the two surfaces:

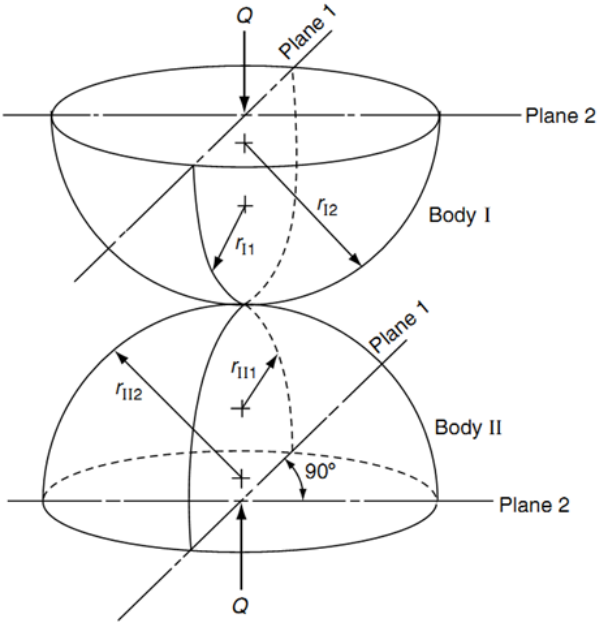

Figure 2.1: Geometry of contacting bodies. Figure from [5]

Curvature sum:

$$\Sigma\rho = \frac{1}{r_{I1}} + \frac{1}{r_{I2}} + \frac{1}{r_{II1}} + \frac{1}{r_{II2}} \tag{2.2}$$

Curvature difference:

$$F(\rho) = \frac{(\rho_{I1} - \rho_{I2}) + (\rho_{II1} - \rho_{II2})}{\Sigma\rho} \tag{2.3}$$

The purpose of this is to simplify the contact problem to an equivalent ellipsoid in contact with a flat plane. From the curvature sum and the sign conversion stated before it is apparent that a concave surface gives a smaller curvature sum, or a bigger equivalent radius, than a convex surface.

The curvature difference describes the shape of the contact ellipsoid. If it is sphere shaped, i.e same radii in both planes, the difference is zero. If it is a cylinder on the other hand, the difference approaches infinity.

The following geometric parameters seen in figure 2.2 are used to calculate the contact deformation. It shows the cross section of an angular ball bearing through a ball with diameter D and the radius of the groove for the inner and outer raceway, r_i and r_o respectively .

From this the osculation of the bearing can be obtained. Osculation is the ratio the radius of the rolling element to that of the raceway in transverse rolling direction and is defined as

$$\phi = \frac{D}{2r}$$

we can then let $r = fD$ and define osculation as

$$\phi = \frac{1}{2f} \tag{2.4}$$

With body I as the ball and II as the raceway, the contact between ball and inner raceway, $F(\rho)$, is then as follows:

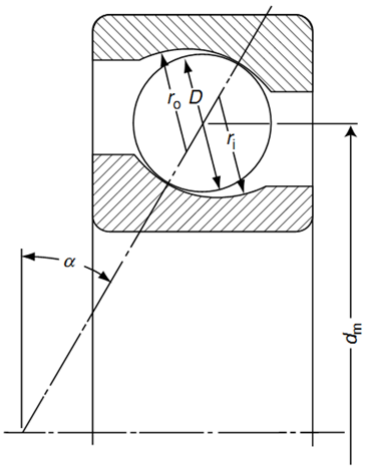

Figure 2.2: Ball bearing cross section geometry. Figure from [5]

$$r_{I1} = r_{I2} = \frac{1}{2}D$$

$$\begin{aligned} r_{II1} &= \frac{1}{2}d_i = \frac{1}{2}\left(\frac{d_m}{cos\alpha} - D\right) \\ r_{II2} &= f_i D \end{aligned} \tag{2.5}$$

By introducing the parameter γ as

$$\gamma = \frac{Dcos\alpha}{d_m} \tag{2.6}$$

into 2.1 and 2.5 we get

$$\begin{aligned} \rho_{I1} &= \rho_{I2} = \frac{2}{D} \\ \rho_{II1} &= \frac{2}{D}\left(\frac{\gamma}{1-\gamma}\right) \\ \rho_{II2} &= -\frac{1}{f_i D} \end{aligned}$$

$$\Sigma\rho_i = \frac{4}{D} - \frac{1}{f_i D} + \frac{2}{D}\left(\frac{\gamma}{1-\gamma}\right) = \frac{1}{D}\left(4 - \frac{1}{f_i} + \frac{2\gamma}{1-\gamma}\right) \tag{2.7}$$

$$F(\rho)_i = \frac{\frac{2}{D}\left(\frac{\gamma}{1-\gamma}\right) - \left(-\frac{1}{f_i D}\right)}{\Sigma\rho_i} = \frac{\frac{1}{f_i} + \frac{2\gamma}{1-\gamma}}{4 - \frac{1}{f_i} + \frac{2\gamma}{1-\gamma}} \tag{2.8}$$

Similarly for the contact between ball and outer raceway, $\rho_{I1} = \rho_{I2} = \frac{2}{D}$ as above; however,

$$r_{II1} = \frac{1}{2}\left(\frac{d_m}{cos\alpha} + D\right)$$

$$r_{II2} = f_o D$$

Therefore,

$$\Sigma\rho_o = \frac{1}{D}\left(4 - \frac{1}{f_o} - \frac{2\gamma}{1+\gamma}\right) \tag{2.9}$$

$$F(\rho)_o = \frac{\frac{1}{f_o} - \frac{2\gamma}{1+\gamma}}{4 - \frac{1}{f_o} - \frac{2\gamma}{1+\gamma}} \tag{2.10}$$

The relative approach of remote points in the contacting bodies are obtained by Harris by solving the complete elliptic integrals describing the contact patch and pressure distribution, arriving in the equation below:

$$\delta = \delta^* \left[\frac{3P}{2\Sigma\rho}\left(\frac{1-\mu_I^2}{E_I} + \frac{1-\mu_{II}^2}{E_{II}}\right)\right]^{2/3} \frac{\Sigma\rho}{2} \tag{2.11}$$

where P is the total load, E the Young's modulus and μ poisson's ratio of the material of the contacting bodies. $F(\rho)$ is always a number between 0 and 1.For radial ball bearings, α is set to zero. δ^* is an dimensionless quantity calculated approximately by Harris and given in table A.1 as a function of $F(\rho)$. The total deformation of the roller is then obtained by summation of the deformation between inner raceway and roller element, and the outer receway and roller element

$$\Delta = \delta_i + \delta_o \tag{2.12}$$

3 Model

When the bearing is mounted it is mostly the local deformations in the contact zones between the rollers and rings that determines the stiffness of the bearing. To model this in a simple but still accurate way, the outer ring of the bearing is made of solid elastic brick elements. All small radii's and geometries like chamfers and roundings are neglected as is usual practice in FE modeling since they do not add any noticeable stiffness to the overall behaviour. By making the outer ring from solid elements, it is easy to implement it in a larger FE-model and the ring can ovalize during loading. It will also be possible to get the pressure distribution on the outside of the ring which will affect the housing in a more correct way than a solid rigid ring or other solutions.

The inner ring is modeled either with solid elastic brick elements in the same way as the outer ring, or as a rigid body connecting the rolling elements to the center of the bearing shaft. Which version to use is optional and decided depending on what kind of analysis the bearing should be used in. If the task is to analyze for example the housing or the displacement of the shaft where the forces in the shaft it self is of no interest, the inner ring will be modeled by a rigid body. This will give a simpler model with fewer nodes and degrees of freedom and therefore a shorter calculation time. If the shaft itself on the other hand is of more interest, the ring will be modeled by solid brick elements.

The ball is then modeled by connector elements, one for radial stiffness and two for axial. Each connector element has a nonlinear elastic behavior represented by a force-displacement curve calculated based on the contact deformations from equation 2.11. The equation first needs to be modified to remove the displacement contributions from the solid

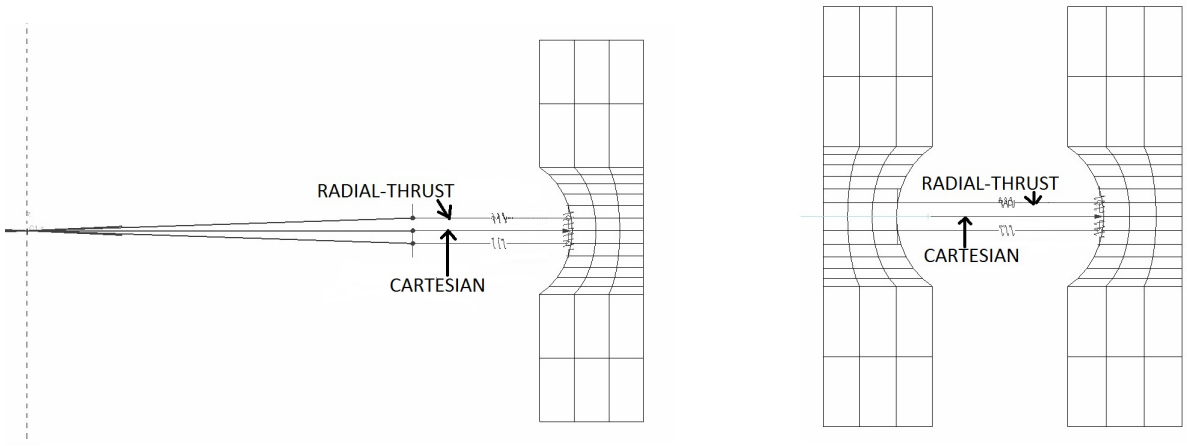

(a) Without inner ring (b) With inner ring

Figure 3.1: Figure showing a cross section with and without FE inner ring

elements in the rings. This is done by considering the ring surface to be rigid, i.e by setting $E_{II} = \infty$ which after simplification leads to:

$$\delta_{rigid} = \delta^* \left[\frac{3Q}{2\Sigma\rho} \left(\frac{1-\mu_I^2}{E_I} \right) \right]^{2/3} \frac{\Sigma\rho}{2} \tag{3.1}$$

Combining equation 2.11 and 3.1 when the inner ring is modeled by a rigid body then leads to:

$$\Delta_{rigid} = \delta_{i,modified} + \delta_o \tag{3.2}$$

and in the second case where the inner ring is modeled by solid brick elements:

$$\Delta_{solid} = \delta_i + \delta_o \tag{3.3}$$

We now have the force-displacement relation for the radial stiffness of the ball during compression, but the balls in the bearing can not transfer any load during tension. To simulate this the curve above the zero displacement line will be vertical (see figure 3.2). For the axial stiffness the equations needs to be modified even further to take in to acount the axial clearance in the bearing. This is done by simply moving the force-displacement curve downwards the same amount as the axial clearance. (again, see figure 3.2). There is also two connector elements for each ball for the axial stiffness. They are connected on each side of the grooves center node so we can simulate a slight movement of the contact zone depending on which direction the axial force is applied in.

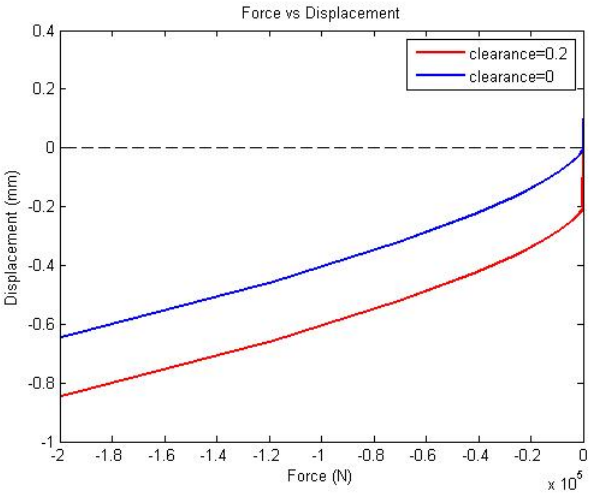

Figure 3.2: Effect of axial clearance on force-displacement curve

4 Script

All keywords used in the following sections can be found in Abaqus user manual [2].

The script starts by reading parameters such as geometry details and desired mesh quality from an input file (Appendix B). It has also an option in the input file to specify if the inner ring should be modeled by either a rigid body or solid brick elements. Based on the parameters from the input file the script creates all nodes in the model with the *NODE keyword. Since a bearing is axis-symmetric it is convenient to first create a cross section of the ring in a local 2D Cartesian coordinate system and then transfer it to a cylindrical coordinate system (figure 4.1 and 4.3), and copy the cross section around the center axis.

4.1 Without inner ring

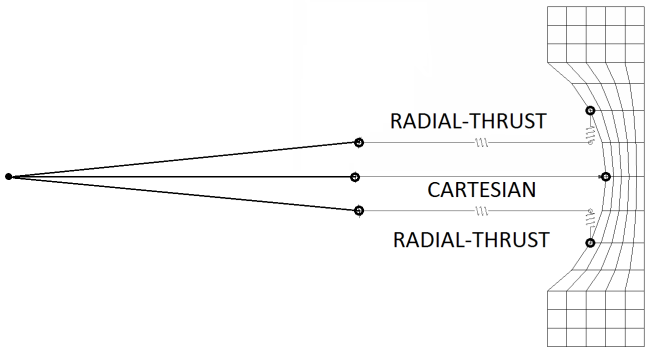

Figure 4.1: Cross-section of RBB showing connection of connector elements with outer ring

The solid elements of the outer ring is then created with *ELEMENT. They are of the type C3D8 (hexagonal first order brick elements). A solid section is then defined for the outer ring to assign material properties to it. On the center node of the groove in figure 4.1 a Cartesian connector element is connected to the rigid body that replaces the inner

ring to act as the radial spring and gap element mentioned in section 3.

For the connector elements that gives the axial stiffness of the bearing, RADIAL-THRUST type is used. They simulate a cylinder where the first node a of the connector element lies on the rotational axis of the cylinder, and the second node b lies on the mantle surface. The radius of the cylinder is decided by specifying the direction of the rotation axis or $\mathbf{e}_3$ in figure 4.2:

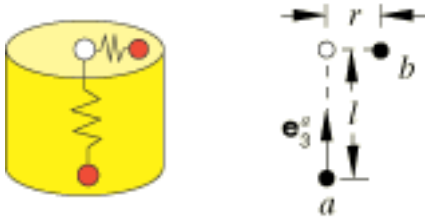

Figure 4.2: Radial-thrust element. Figure taken from [2]

The good thing with the radial-thrust element is that it can have different stiffness in axial and radial direction. This makes it possible to set the axial stiffness to zero and still maintain the perpendicular relation between node a and b seen in figure 4.2.

Between the load center of the bearing and the connector elements a *RIGID BODY is defined which ties the nodes where the connector elements attach to the inner ring with rigid constraints to the bearings center node. The last thing the script does is to create a surface set for the bearing seats to make it easy to find the surfaces and use them in contact pairs in a system analysis

4.2 With inner ring

When the option to model the inner ring as solid elements instead of a rigid body, there is only small differences in the script. The ring itself is modeled just like the outer ring with C3D8 elements, and the connector elements are connected to the corresponding nodes on the inner ring (see figure 4.3). When the inner ring was made of a rigid body, the rotation of the nodes where the connector elements are attached is automatically locked because the rigid body share all degrees of freedom with the reference node, which in this case is the bearings center node. Solid brick elements on the other hand does not constrain any rotations in the nodes. This allows the connector element to rotate which creates convergence problems. To keep this from happening a layer of shell elements is created on the inner rings groove surface to lock the rotations. The rest of the script is the same as previous section.

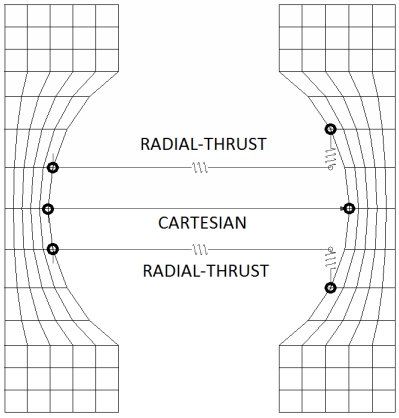

Figure 4.3: Cross-section of RBB showing connection of connector elements between inner ring and outer ring

5 Evaluation

A radial ball bearing is designed to transfer load primarily in radial direction. It can transfer some load in axial direction but in most applications there is a tapered roller bearing or an angular roller bearing that takes most of the axial load and our bearing is thus tested only for radial load.

5.1 Stiffness validation

To test the stiffness of the bearing model it was compared against an experimental test performed by El-Sayed [3] on two SKF series 62 bearings (6205 and 6209). The test was performed by fixing the bearing in a base block which covered the bottom half. A 80 mm long shaft was attached to the bearing bore and load was applied on the shaft using a universal testing machine. The load on the bearing and the movement of the shaft was recorded. To get the correct bearing deflection the corresponding shaft deflection was subtracted from the measured shaft deflection. The setup is shown in figure 5.1.

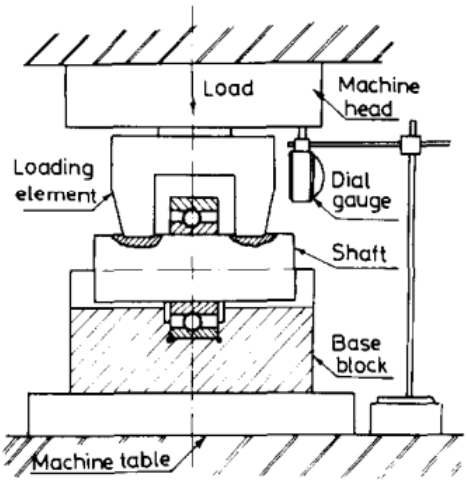

Figure 5.1: Experimental test setup. Figure from [3]

To compare the test data with our models a bearing with rigid inner ring and 2100

solid elements was used. The outside nodes of the bottom half of the ring was locked in x-, y- and z-direction. A load was then applied at the center node in radial direction. The setup is shown in figure 5.2.

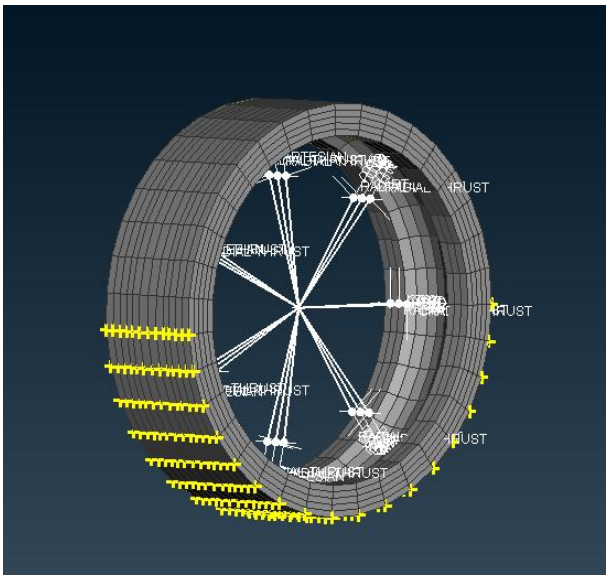

Figure 5.2: Setup for radial stiffness measuring

The measured results are shown in figure 5.3. λ is the stiffness coefficient of the applied load divided by the resulting deflection of the bearing center with the unit kN/μm. The 6205 bearing has an outer diameter of 52 mm, and inner diameter of 25 mm, the 6209 bearing is 85 mm and 45 mm respectively.

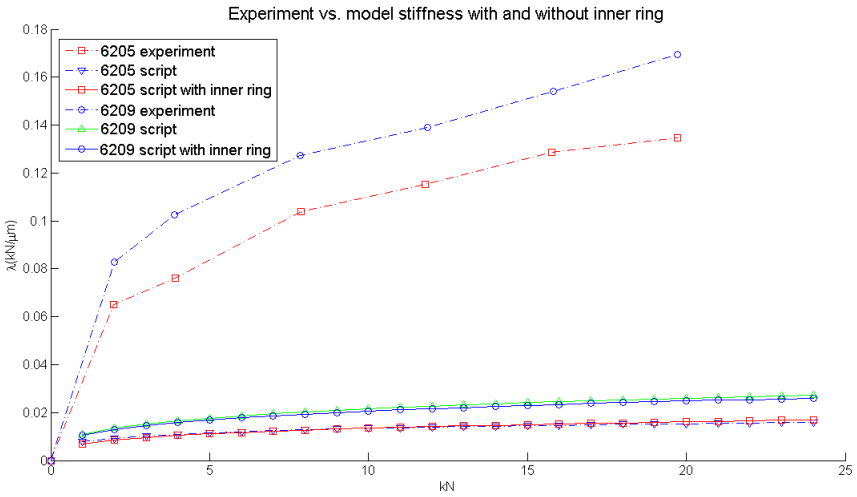

Figure 5.3

As can be seen, the stiffness of our models are much lower than the measured SKF bearings. This is probably because the springs are connected to only one node which will effectively transfer the load in the rolling elements to one consentrated point on the race-way surface instead of an area. To verify this a bearing with solid FE bearing balls (Figure 5.4) were modeled and the stiffness compared to the experimental values (Figure 5.7). This model has a slightly higher stiffness then the experiment, but it is still much closer then the stiffness of our script. A section of the bearing through the center of one of the bearing balls

were then made in both the script model and the one with solid balls when 4 kN was applied on them (Figure 5.6). In this section it is clear that the displacement in the node where the spring is connected is much higher than it should be compared to the solid bearing ball.

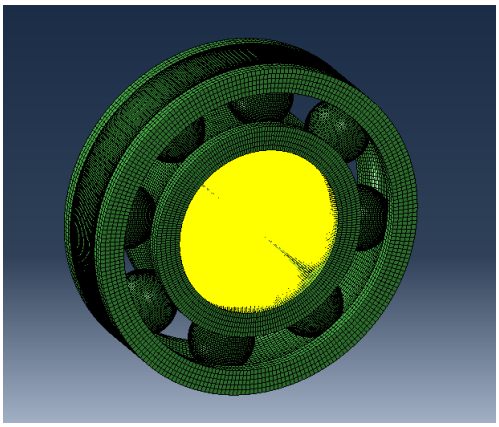

Figure 5.4: Bearing with solid balls

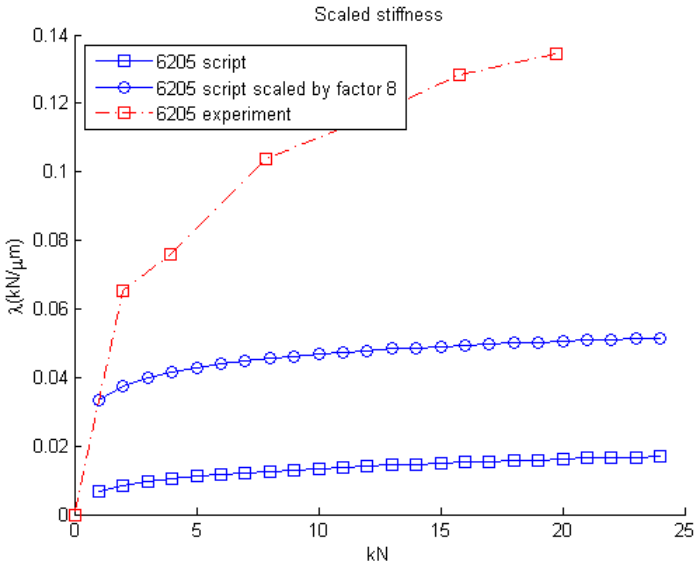

Figure 5.5: Stiffness of bearing scaled by a factor of 8

Another problem is also that even if the stiffness of the springs would be scaled by a factor to compensate the low stiffness in the rings, it is not enough since the contact area also needs to increase as the load increases. As it is now the solid elements will behave linearly and thus reduce the nonlinear behavior of the complete bearing. This can be seen in figure 5.5 where the spring stiffness is increased by a factor 8. The curve is only translated upwards, but the shape is not changed.

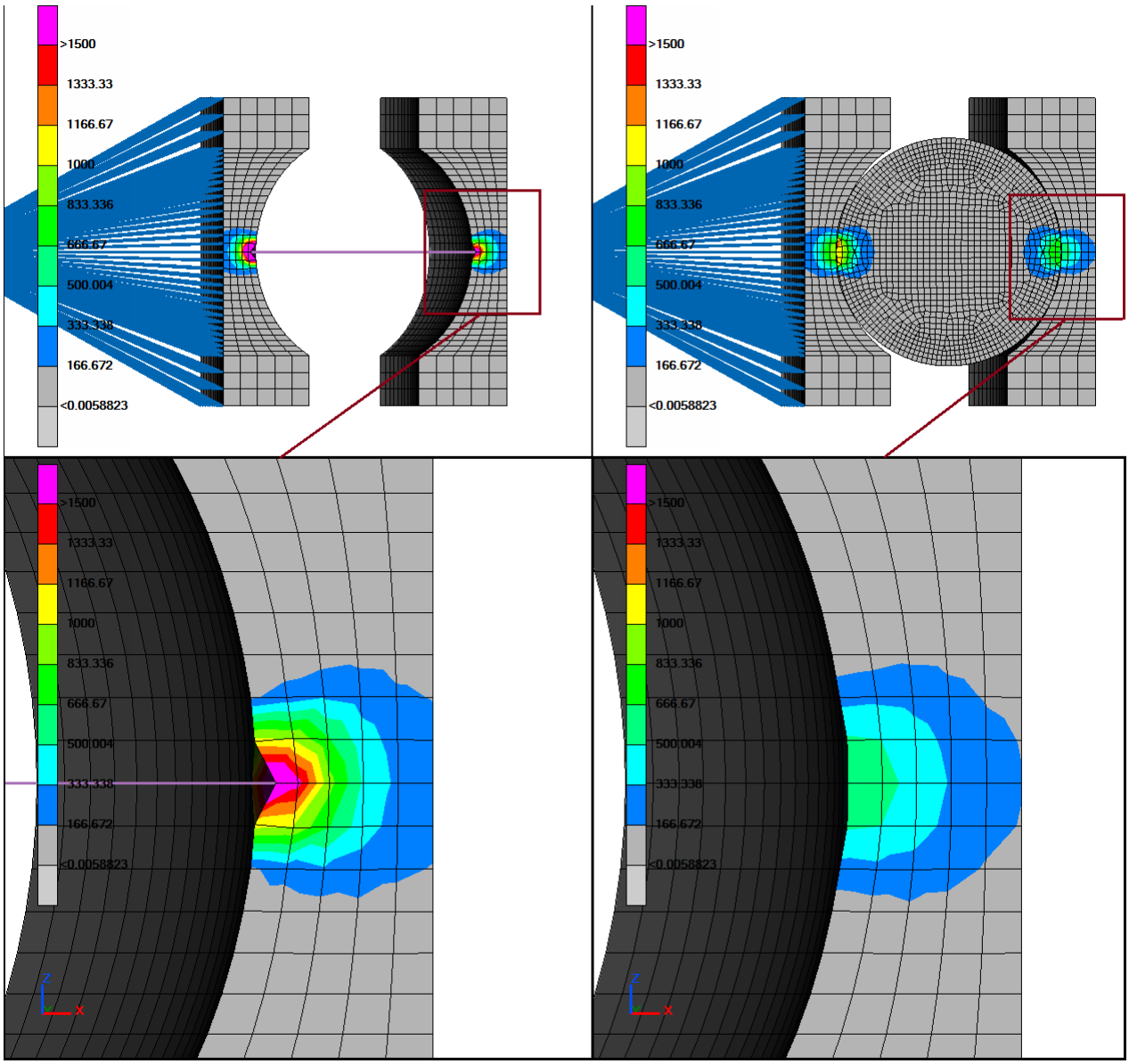

Figure 5.6: Comparison of a crossection through a rolling element of our model and a ball made of solid elements. The solid ball is hidden in the zoom-in view in the bottom right corner, and the deformations are scaled by a factor 5.

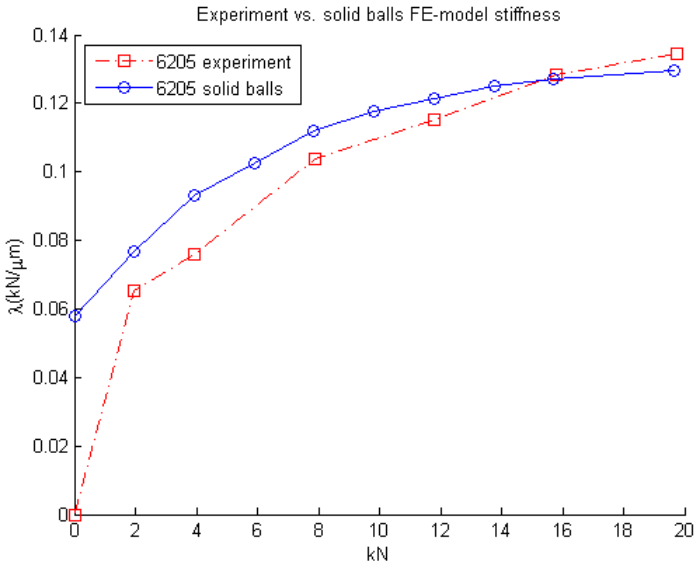

Figure 5.7: Stiffness of bearing with solid balls

5.2 Mesh dependency and rigid versus solid inner ring

To see how the mesh size and the two ways to model the inner ring affects the stiffness of the bearing the same setup as in previous section was used again. Four bearing versions were tested, all of them with the dimensions of a SKF 6205 bearing. With rigid inner ring we had one with 2100 elements and one with 16 800 elements, with solid inner ring we had 4200 and 33 600 elements. The results are shown in figure 5.8.

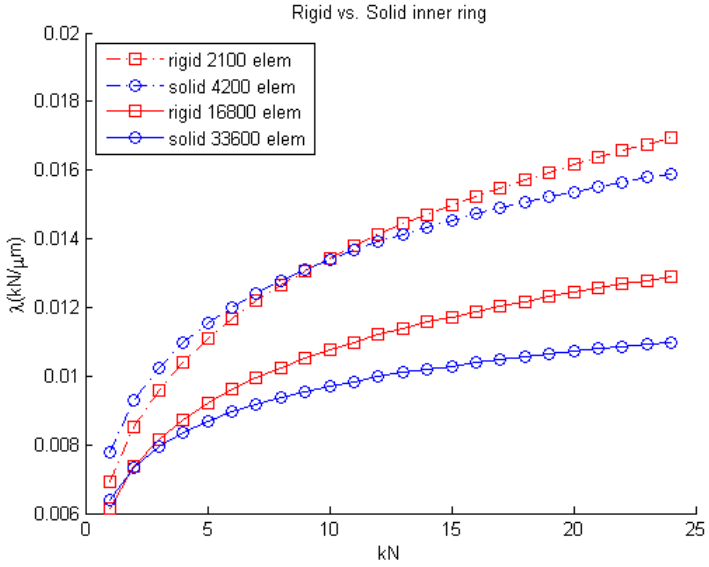

Figure 5.8

As can be seen, the effect from previous section were the solid elements reduce the stiffness and non-linearity behavior of the bearing, increases when the number of elements is increased, i.e. when the element size is reduced. It is also worth noting that the difference between using a rigid or solid inner ring is fairly small for the coarse mesh but bigger for the fine mesh and that the solid ring is weaker than the rigid.

5.3 NLGEOM and eigenfrequency

To check the stability of the bearing model a system with a crown wheel and pinion gear containing four bearings were simulated first with NLGEOM on and then as an eigenfrequency test. NLGEOM is a setting that allows for large deformations in all six degrees of freedom. The results themselves were of little interest since there was no experimental data to verify them against. Instead the test was done to see if they would converge at all and test the stability and speed of our models and see if they would work in simulations in the future.

Both options ran smoothly and gave reasonable results. The NLGEOM run was also compared with a standard simulation of the same model and the results were the same in both cases which is expected if they work correctly.

5.4 Mesh dependency check for spokes pattern model

In order to implement the model directly in a system analysis it is important to verify that results are independent of the mesh. Test were made with three different element sizes; 0.5 mm, 1 mm and 2 mm. Different element size gives different number of solid elements in the bearing ring which in turn gives different number of springs in the bearing. Because

of this the stiffness of the springs has to be adjusted to maintain the same global stiffness of the bearing for each model. The results can be seen in figure 5.9.

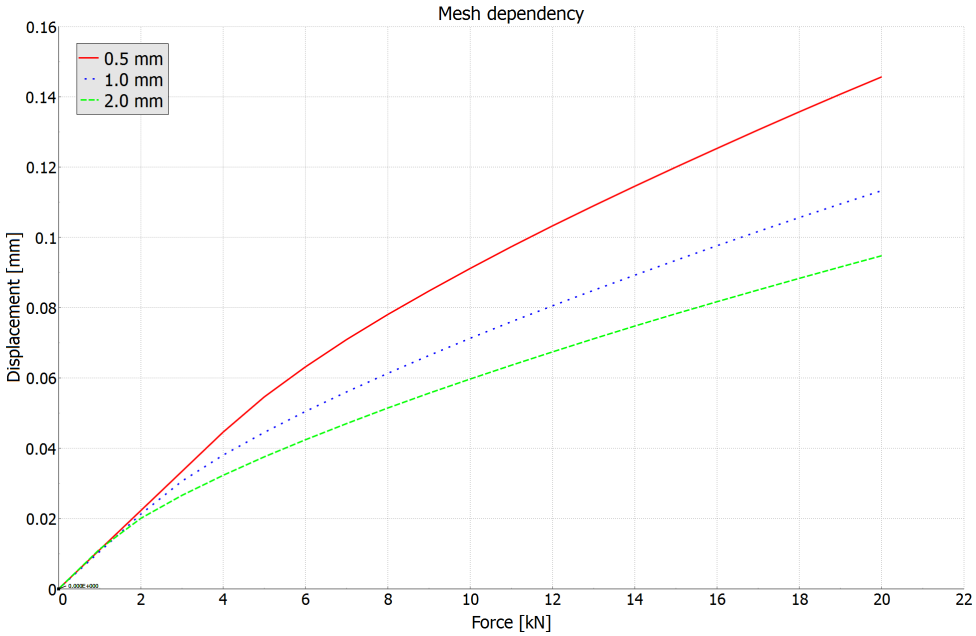

Figure 5.9: Mesh dependency check.

The stiffness of the springs is reduced based on geometric data. This method does not gives satisfactory results for small element size. More springs gives a larger displacement, and the correction factor is therefore to large. The detailed contact analysis has to be carried out with solid rollers in order to understand the contact mechanics.

FE-model and experiment data shows a good correlation when using 2 mm element size. The FE-model is too stiff at low loads but matches the experiment well above 7 kN load, see figure 5.10.

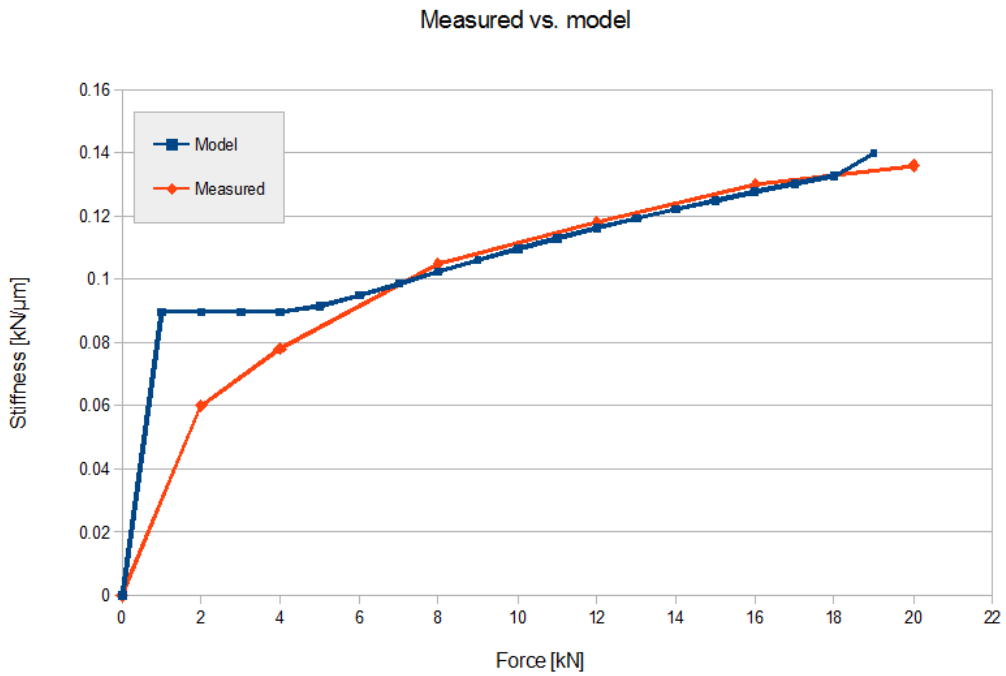

Figure 5.10: Correlation of stiffness between experiment results and FE-model.

6 Conclusions

The overall results is a well working script that generates an arbitrary radial ball bearing from an input file containing all necessary dimension and mesh parameters. For the final user in need of a bearing model to use in a bigger FE-model the amount of work is considerably reduced. The model is stable and has good and fast convergency.

The stiffness of the model however is not yet satisfactory and needs improvement. As mentioned in section 5.1 and seen in figure 5.6, the low stiffness is probably because the springs are connected in only one node on the raceway. This can be seen by comparing the stiffness of the model with solid balls which have a stiffness much closer to the experimental bearing (figure 5.7). Because of this it is not possible to capture the effect of the growing elliptical contact zone between the rolling element and bearing raceway when the load is increased. One way to fix this problem could be to instead of attaching the spring representing the rolling element directly to the center node of the groove, connector elements could be inserted in a spokes pattern between all the nodes in the groove and the spring. Each connector element would then have a force displacement curve simulating a rigid body and gap element in series where the gap would have the same distance as the actual distance between the groove and ball at the node position where it is attached. This would only give a growing contact zone in the plane shown in figure 2.2. The effect in this plane though is higher than the plane perpendicular to it because the radius difference between the ball and groove is much smaller, and would probably be enough to give a satisfactory result. It is hard to estimate how much a solution like this would increase the computation time, but since there is no contact involved the time should not increase more then a fef percentages.

Another way of solving the problem could be to add a rigid surface with the shape of the ball which the spring would be connected to. However, this would require a contact definition between the solid ring elements and the rigid surface which would increase the

calculation time quite significantly and also make the model more unstable compared to the solution mentioned above, especially for high axial loads where sliding between the raceway and rigid surface could occur.

The results from section 5.2 where the mesh dependency and rigid versus solid inner ring is tested suffers from the same problem mentioned for the stiffness, i.e. that the contact zone is not a zone but a point. If the contact zone would be made in to an area by spreading out the load with the extra connector elements suggested, the difference in stiffness for the different mesh sizes would probably disappear as well.

7 Future work

When a correct stiffness is obtained, the possibility to use the bearing in a thermal analysis should be added. The way it is now there will be strains in the bearing when the other components in an FE-model expand and the bearing is not. This is easily implemented for the solid element by just adding a thermal expansion factor in their definition, but the other elements needs to be investigated more to understand how this could be added.

Second priority would be to add an option to use solid elastic second order brick elements instead of first order elements. This would give a higher freedom when choosing which surface in the contact between the bearing and housing or shaft that should be master or slave surface in ABAQUS contact pair definitions. This is because the surface with the coarser mesh should act as the master surface which in most cases would be the bearing. But in a large FE-model you would like to have the housing as the master surface so you would then have to increase the number of elements in the bearing to get a finer mesh which would increase the computational cost. If the solid elements of the bearings instead is of second order you can still have a relatively low number of elements and have the bearing act as slave surface. To extend or do a new similar script that can automatically generate a tapered roller or angular contact ball bearing is also wanted.

References

[1] Peng Chunjun. Static analysis of rolling bearings using finite element method. Master's thesis, Universität Stuttgart, 2009.

[2] Dassault Systèmes. *Abaqus 6.10 Online Documentation*, 2010.

[3] H. R. El-Sayed. Stiffness of deep-groove ball bearings. *Wear*, 63:89–94, 1980.

[4] Hermann Golbach. Integrated non-linear femodule for rolling bearing analysis. *INA reprint "Proceedings of NAFEMSWORLD CONGRESS '99 on Effective Engineering Analysis"*, 2, 1999.

[5] T. A. Harris. *Rolling Bearing Analysis.* John Wiley & Sons Inc., forth edition, 1986.

[6] H. R. Hertz. Uber die Berührung fester elastischer Körper und uber die Härte. *Verhandlungen des Vereins zur Beförderung des Gewerbefleisses*, 1882.

Appendices

A Dimensionless contact parameters

Table A.1: Dimensionless contact parameters

$F(\rho)$	δ^*
0	1
0.1075	0.9974
0.3204	0.9761
0.4795	0.9429
0.5916	0.9077
0.6716	0.8733
0.7332	0.8394
0.7948	0.7961
0.83495	0.7602
0.87366	0.7169
0.90999	0.6636
0.93657	0.6112
0.95738	0.5551
0.97290	0.4960
0.983797	0.4352
0.990902	0.3745
0.995112	0.3176
0.997300	0.2705
0.9981847	0.2427
0.9989156	0.2106
0.9994785	0.17167
0.9998527	0.11995
1	0

B Input file

```
BEARING NAME:
<BearingA>

-------------------------------------------------
        OUTER RING
-------------------------------------------------

BEARING OUTER RING MESH PARAMETERS: (   Nr of radial elements,
                                        Nr of axial elements outside groove,
                                        Nr of axial elements within groove,
                                        Nr of elem between balls)

<5,6,6,5>


BEARING OUTER RING GEOMETRY: (D, D_groove, d, d_groove, alfa, B, nr, r)
<62, 52.858, 30, 38.954, 60, 16, 8, 5.55>

D:              outer ring diameter
D_groove:       outer ring groove diameter
d:              inner ring diameter
d_groove:       inner ring groove diameter
alfa:           angle of attack
B:              axial width
nr:             number of balls
r:              radius of balls


-------------------------------------------------
        INNER RING
-------------------------------------------------

USE INNER RING: (0 = no, 1 = yes)
<0>

BEARING INNER RING MESH PARAMETERS: (   Nr of elements radially,
                                        Nr of axial elements outside groove,
                                        Nr of axial elements within groove )

<5,6,10>

BEARING STIFFNESS PARAMETERS: (E, nu, scale)
<210e3, 0.3, 1>

E:                Elasticity modulus, [MPa]
nu:               Posions ratio
scale:            Stiffness scale factor
c@FancyVerbLinee  Stiffness scale factor
```